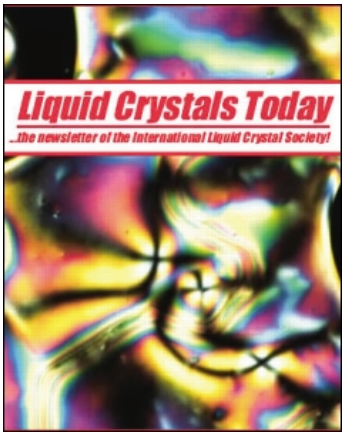

Liquid Crystals Today
Publication details, including instructions for authors and subscription information:
http://www.informaworld.com/smpp/title~content=t713681230

Liquid Crystals — as seen by the Scanning Tunnelling and Force Microscopes

Jane Frommer[ab]
[a] IBM Almaden Research Center, San José, CA, USA [b] Institut für Physik, Universität Basel, Basel, Switzerland

To cite this Article Frommer, Jane(1993) 'Liquid Crystals — as seen by the Scanning Tunnelling and Force Microscopes', Liquid Crystals Today, 3: 2, 1 — 12
To link to this Article: DOI: 10.1080/13583149308628615
URL: http://dx.doi.org/10.1080/13583149308628615

Newsletter of the International Liquid Crystal Society

LIQUID CRYSTALS Today

Vol. 3, No. 2 July 1993

Liquid Crystals — as seen by the Scanning Tunnelling and Force Microscopes

by Dr Jane Frommer, IBM Almaden Research Center, San José, CA 95120, USA, and Institut für Physik, Universität Basel, Klingelbergstrasse 82, 4056 Basel, Switzerland.

Liquid crystals have provided an invaluable service for the development of the scanning tunnelling microscope (STM). In return, the STM has done well for liquid crystals. What is meant by this anthropomorphising of scientific techniques and materials? The technique of STM was originally confined to the study of metallic surfaces by the belief that only intrinsically conducting materials could be successfully imaged. Then liquid crystals were imaged with stunning clarity. They served as well-behaved subjects that proved unambiguously that the STM could image organic molecules. Their tendency to self-assemble into immobilised planes and their readily recognisable molecular moieties facilitated recording and interpretation of images. Those images are the subject of this overview of STM and AFM (atomic force microscope) studies of molecular ordering in liquid crystal arrays [1].

Introduction to the Scanning Tunnelling and Force Microscopes (STM and AFM):

The new imaging technique of STM enables direct atomic-scale measurements to be made from data collected not from an average over many atoms, rather recorded locally, atom by atom. [1]. The operating principle of STM is an electrical current that flows between two conductors, configured as a scanning tip and a stationary planar electrode (Fig. 1). The two are separated by a very thin electrically insulating layer (typically angstroms) through which the electrons "tunnel". In the case of imaging molecules such as liquid crystals, the organic molecules are configured as adsorbates on the planar electrode and serve as the thin insulating layer. As the tip is scanned over the surface, the tunnelling current is collected from a series of points, angstrom by angstrom, i.e. at an atomic scale. When this atomic information is pieced together laterally, like the pieces of a puzzle, an image of the whole surface is obtained, be it the face of a crystal lattice or the backbone of a hydrocarbon chain. In cases of homogeneous materials, such as a single crystal metal, this current map reflects the surface topography, with atoms appearing as "hills" of higher current and the area between them appearing as "valleys" of lower current. In cases of organic adsorbates, the contours of the current map correspond to the features of individual molecules, The actual mechanism by which the electrons tunnel through the organics to produce current maps that correspond to molecular geometries remains an open issue.

An AFM is similar to an STM in that a sample surface is scanned by a probe (Fig. 1). The monitored interactions are not based on electrical current however; instead they arise from attractive or repulsive interactions between probe and sample. These interactions (dispersion, magnetic, electrostatic etc.) are manifested as small motions of the probe that are recorded with a detector, typically an optical beam. An x,y plot of these locally recorded motions provides a map of surface interactions, interpreted as surface topography. Because the region on the tip that interacts with the sample is usually several square

(Continued on p 5)

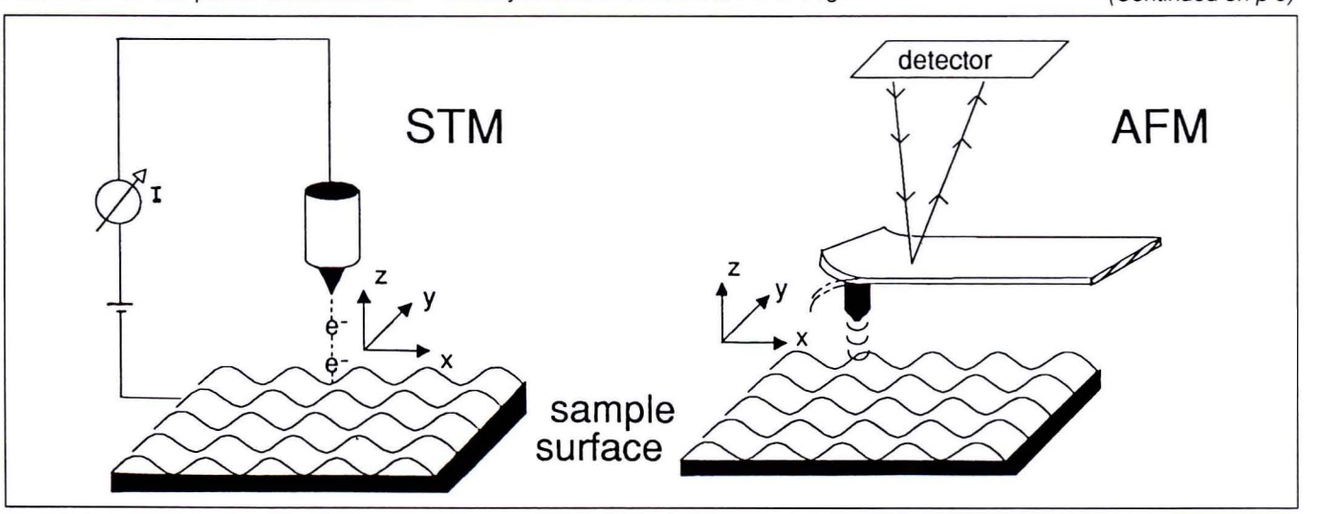

Fig. 1. Schematic illustration of the STM and AFM instruments highlighting their common feature of a localised probe that scans a surface composed of atomic or molecular features and collects data directly over very localised sites of angstrom or nanometre dimensions.

Liquid Crystals — as seen by the Scanning, Tunnelling and Force Microscopes

(continued from front page)

nanometres, resolution in AFM images is of the order of nanometres. Future developments in AFM tip design will improve the resolution of AFM images towards the level obtained in STM.

Most of the scanning microscope studies of liquid crystals have been obtained with the STM. Sample preparation involves deposition of the organic adsorbate onto the conductive substrate (e.g. graphite or MoS_2) by a variety of deposition techniques: sublimation, adsorption from solution, melting or application of a neat liquid. Regardless of the preparation technique, the STM is sampling only the layer or layers closest to the interface with the conducting substrate.

It can take from several seconds to several minutes to record an image, depending on the scan size, the surface roughness, and the level of resolution. Most STMs are operated at room temperature, although instruments have been customised to operate at variable temperatures. For example, a smectic-to-isotropic phase transition has been induced in a liquid crystal by the scanning action of the STM tip at temperatures above the bulk S-I temperature [2].

Since present scanning and imaging methods require immobilising the molecules so that they are not continually displaced by the action of the scanning tip, the characteristic behaviour of liquid crystals to form ordered phases makes them ideal objects for STM investigations. The ability of the STM to focus on the monolayer(s) closest to the substrate provides new information on the role of the substrate in affecting intermolecular order, long- and short-range, where the driving force for assembly comes from both intermolecular and surface-substrate interactions.

A well studied class of Liquid Crystals: Alkylcyanobiphenyls

The first use of the STM to study the ordering of liquid crystals on graphite was published in 1988 [3]. The initial material studied, 4-n-octyl-4'-cyanobiphenyl (8CB), has since proved to be especially popular in continuing STM studies of organic adsorbates [1].

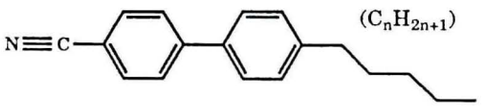

Fig.1 *Alkylcyanobiphenyls (nCB), extended (all trans) structures*

STM images of 8CB on the graphite basal plane have been collected on various scales, from 'large' areas over microns to smaller areas over several angstroms [1]. In larger scans, the long-range ordering of molecules is evidenced as rows, 38Å wide and extending for hundreds of angstroms (Fig. 2a). Occasionally these rows are observed to terminate at boundaries (Figs. 3a, b) that originate either in the organic layer or in the underlying substrate *(vide infra)*.

On narrowing the scan to 112 x 112Å² and then to 57 x 57Å², the rows are resolved to be made up of parallel molecules, (Figs. 2b, c). The cyanobiphenyl head group has the appearance of a brighter oval, while the alkane tail appears as a fainter chain (areas of higher and lower current, respectively). Each row interacts in amphiphilic fashion with neighbouring rows: head-to-head and tail-to-tail.

From these images it can be seen that the molecules are lying down on the graphite surface, as opposed to extending their long axes normal to the substrate plane (Fig. 4). The rows are subdivided into discrete packets of molecules, each packet, or unit cell, containing eight molecules. Each consecutive unit cell is laterally offset 7Å from its neighbouring cell within the row. This periodic offset, every eight molecules, is possibly a mechanism by which strain from incommensurate packing in the substrate is relieved. Close examination of the angle formed by the biphenyl group and the alkyl group reveals a progressive increase in angle, from ~12° to ~35° on going from the first to the fourth molecule on one side of the unit cell (better discerned in Fig. 6). In images like these of phenyl groups which resolve as actual ring-like structures, the rings are considered to be lying down flat on the substrate. The position of the cyano group can

Fig. 2: STM images of 8CB on a graphite substrate

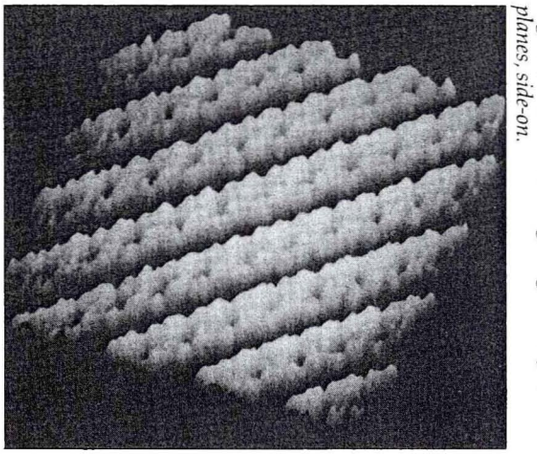

Fig 2a: *(250 x 250Å²) Long-range order of smectic planes, side-on.*

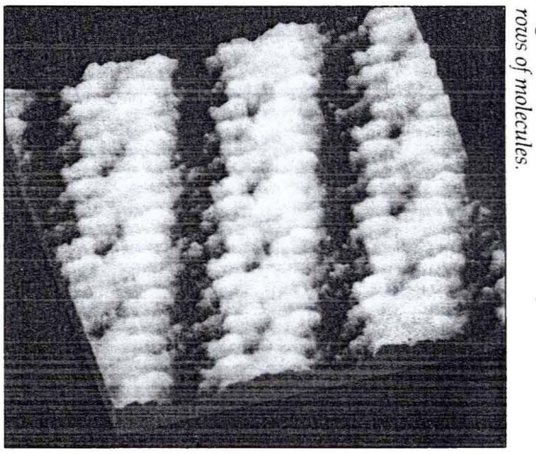

Fig 2b: *(114 x 114Å²) Smectic layers resolved as rows of molecules.*

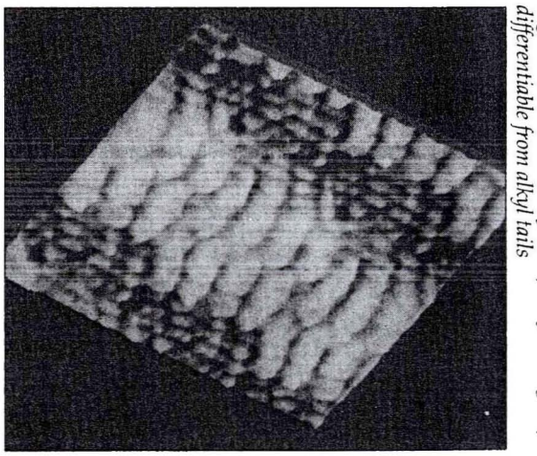

Fig 2c: *(57 x 57Å²) Cyanobiphenyl headgroup differentiable from alkyl tails*

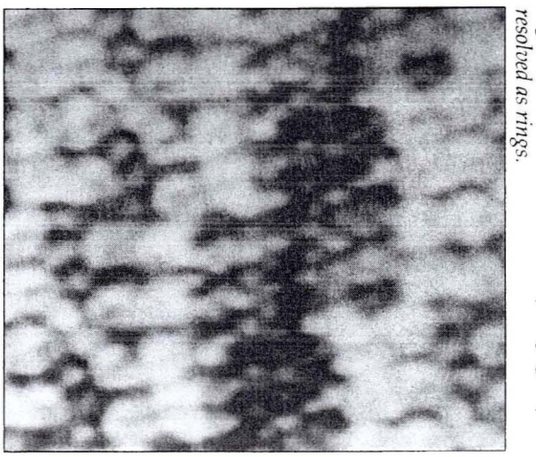

Fig. 2d: *(57 x 57Å²) Individual phenyl groups resolved as rings.*

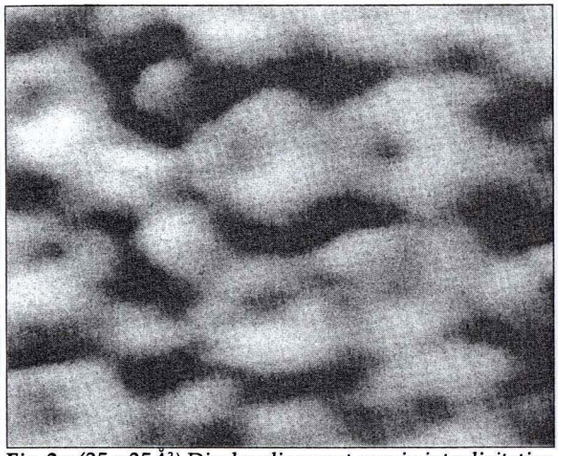

Fig. 2e: *(25 x 25Å²) Dipolar alignment seen in interdigitation of nitrile groups.*

also be seen as a bright spot off the phenyl ring, para to the biphenyl linkage. One of the most outstanding features of these STM images of 8CB is illustrated in Fig. 2e, a scan area focused on the interaction between vicinal headgroups (25 x 25Å²). Figure 2e provides a direct view of interdigitation: by interdigitating neighbouring cyano groups, in opposing directions, electrostatic repulsions between the dipoles of the cyano groups are reduced (Fig. 5). This alignment strives to "cancel" the dipole moment of the nitrile (C=N) group. Dipolar alignment has been considered a major driving force in the assembly of cyano-containing liquid crystals [5]. Now, with the STM, it can actually be visualised, molecule by molecule. In images like that of Figure 2e, the power of the STM as a tool in characterising intra- and intermolecular order is clearly demonstrated [4].

Systematic studies of nCB homologues

Many of the nCB molecules studied to date by STM order similarly on graphite. For example, both decyl (10CB) and dodecyl (12CB) derivatives pack in extended rows, two molecules wide (Fig. 6), with the same head-to-head orientation seen for 8CB [4]. These rows are derived

Fig 3: STM images of boundaries

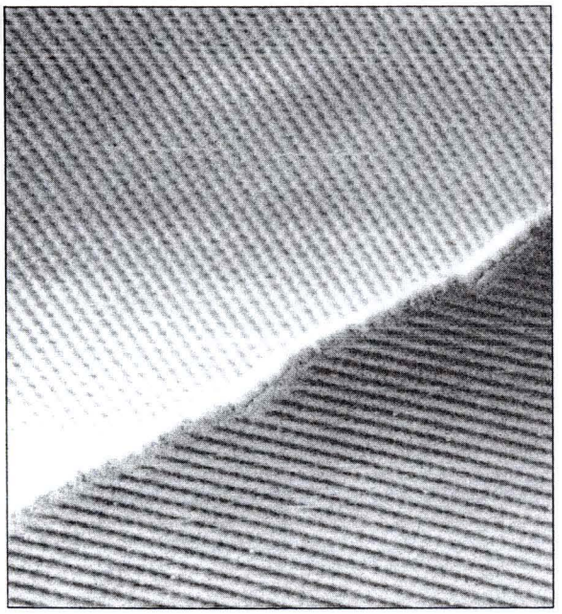

Fig 3a: *(1350 x 2600Å²) 10 CB on graphite with a step height of 3.5Å (one layer of graphite).*

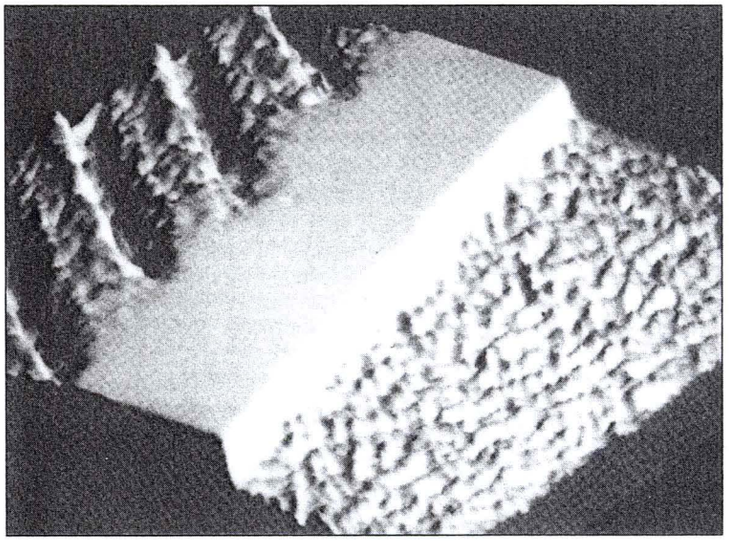

Fig. 3b: *(150 x 150Å²) 8CB on graphite, the termination of a smectic plane at a step edge of ~10 Å. The contrast in this image is adjusted to optimise resolution of the molecular rows on the upper plane, so the higher central section of the image is out of the range of the STM electronics. The lower plane is imaged in the following image, Fig 3c, with scanning parameters optimised for that level.*

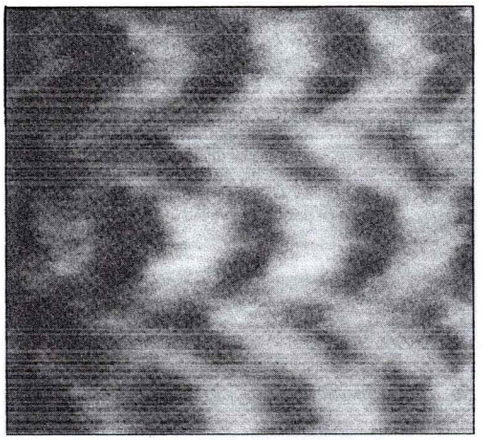

Fig. 3c: *(105 x 105 Å²) The lower plane of the previous image (Fig 3b), brought into better resolution, revealing a moiré pattern for the packing of 8CB on graphite [1].*

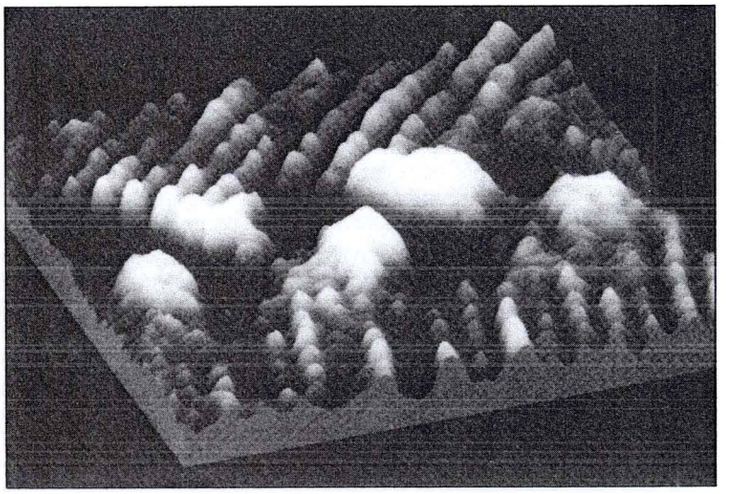

Fig. 3d: *(72 x 72Å²) PCH5 on graphite, with a boundary between two domains orientated 30° to each other [3].*

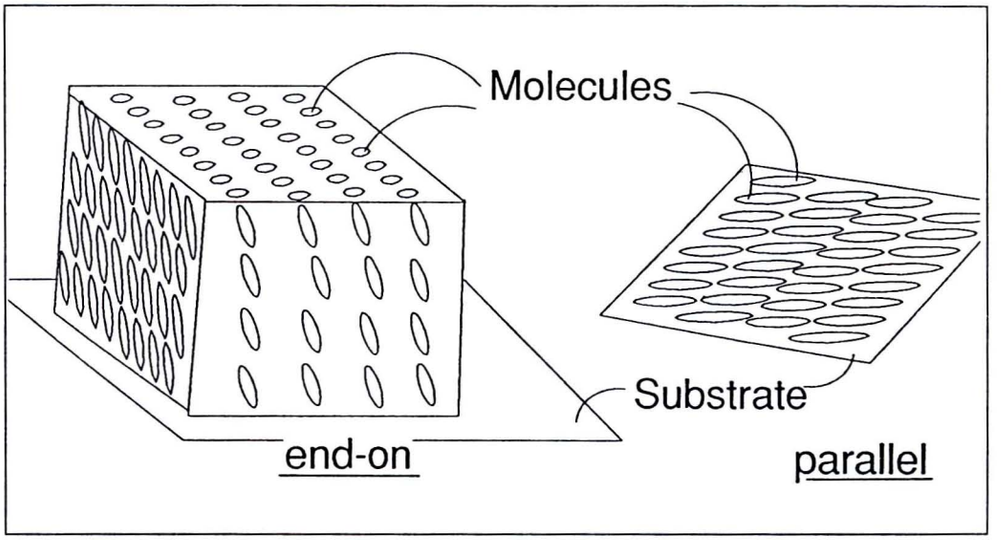

Fig. 4: Schematic representation of molecular orientation on a substrate, for the classes of molecules discussed in the text. The end-on conformation imaged in the AFM studies of LB films and the parallel conformation is imaged in the STM studies of liquid crystals.

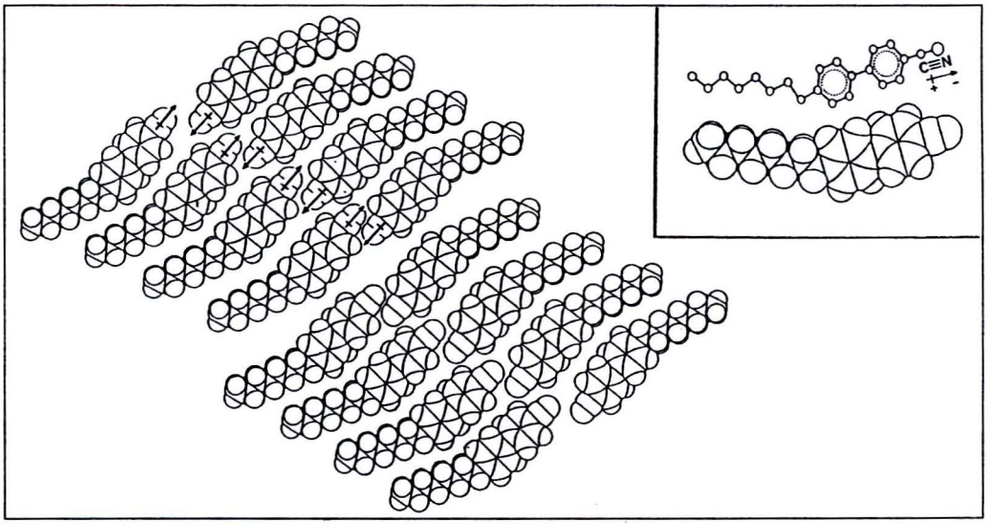

Fig. 5: Cartoon depicting the cyanobiphenyl molecules as they are commonly seen to align in the STM images. The alignment of nitrile dipoles is highlighted.

from smectic planes, viewed side-on. Actually, their degree of order is more crystalline than smectic, with very regular correspondence between rows as well as within the rows. Whereas it is more accurate to refer to the patterns viewed in these picture as two-dimensional crystals, the tendency has been to borrow traditional nomenclature in describing molecular orientation in the STM images.

In comparing cyanobiphenyls of different alkyl chain lengths, a comfortable linear relationship is recorded between increasing alkyl chain length and increasing (smectic) row spacing [4] (See graph). For example, the width of the "unit cell" of eight molecules in 8CB, measured from the terminal methyl group, across the interdigitated heads to the terminal methyl group of the opposing molecule, is 38Å. An analogous measurement on 10CB, the decyl derivative with two more methylene (CH_2) units per molecule, yields a unit cell width of 43Å. Extension to 12CB, produces a 47Å width. The step-wise increases of 4-5 Å on going from octyl to decyl to dodecyl derivatives corresponds with a predictable increase in chain length of 1.25Å per methylene unit (Note: there are two molecular lengths per row width).

Extension of the series in the opposite direction, to shorter chain lengths, results in more changes than just narrowing of the widths of the rows [1]. The hexyl derivative 6CB, forms a pattern of long rows of parallel molecular axes and head-to-head contact; however it differs from the other nCBs in the orientation of phenyl rings relative to the underlying substrate (Fig. 7). With 6CB, every second biphenyl unit appears to be canted, wedged between its two adjacent biphenyl neighbours which are lying flat. The hexyl tails in these images are less obvious than their higher molecular weight homologues, perhaps due to thermal motion.

Since 6CB, 8CB, 10CB, and 12CB all share a common head group structure, the cyanobiphenyl unit, one looks to the influence of the tail in explaining the differences in their images. The principal change on proceeding down to the hexyl derivative in the cyanobiphenyl series is the further shortening of the alkyl component by two methylene units (~2.5Å), from the dodecyl (C12) to the decyl (C10) to the octyl (C8) and finally to the hexyl (C6) derivative. Thus, the rather major difference in the position of the C6 molecules on the surface indicates that n=hexyl is below a threshold of the alkyl group's influence on (a certain degree of) ordering of the nCB molecules. The lack of well-ordered tails in 6CB perhaps releases the constraint on the phenyl head groups to accommodate alkyl tail intermolecular spacing. (The width of an alkyl chain is ~ 4Å and the width of a flat-lying phenyl ring is ~5.4Å). The lower observed order in the hexyl chain is consistent with the fact that bulk 6CB is in the nematic at room temperature, the temperature of the STM experiments, whereas the others are in the more highly ordered smectic phases.

7CB, has an alternate packing for the nCBs on graphite [6]. This packing mode is also observed on rare occasions with 8CB on graphite (Fig.9) and with some nCBs on other substrates *(vide infra)*. 7CB also deviates from the higher molecular weight nCB analogues discussed above by having an odd number of carbons in the alkyl moiety, subjecting it to odd/even alternation affects often observed for alkanes. Like 6CB, 7CB is a room temperature nematic in the bulk. Measurements of smectic layer spacings by STM are compared to X-ray and neutron scattering [5] results. On average, the latter are 1.2 times greater than the STM-measured

Smectic layer spacing vs. tail length in nCBs. The STM data are from ref. [4] and the X-ray data are from ref. [5].

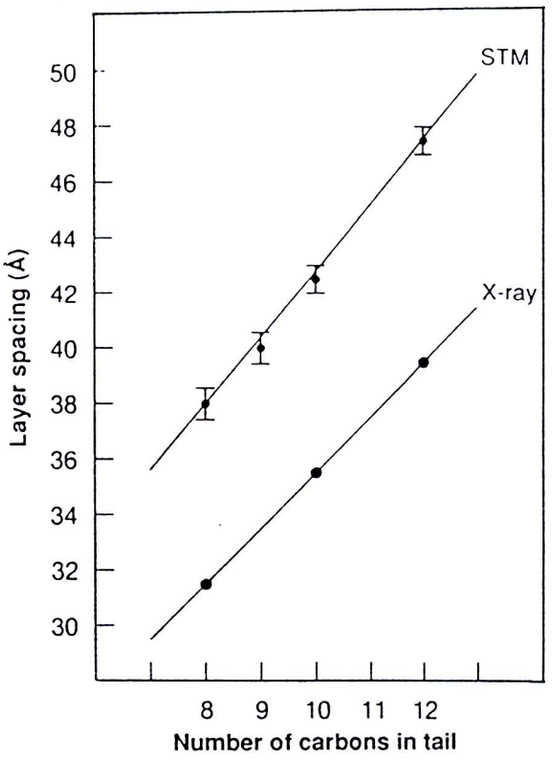

spacing for 8CB, 10CB, and 12CB (see Graph [4, 5]). This discrepancy is not surprising when the molecules' environment is considered: X-rays and neutrons interact with molecules in the bulk, i.e. molecules that are surrounded by like molecules. The STM, however, measures molecular spacings in a layer of molecules located at the 'edge' of the bulk, at the interface with a substrate. The factor of 1.2 is probably due to the influence of the substrate on the ordering of the proximal organic adsorbate, such as lattice mismatch. The shorter smectic spacing detected by X-rays on the bulk could be due to a number of molecular origins, e.g. less extended alkyl tails. This example of a notable difference between results obtained from the bulk and from the interface reinforces the caution that must accompany interpretation of STM images. Direct extension of phenomena and principles from the bulk to the angstrom scale at interfaces could be misleading.

Substrate effects: Graphite as a substrate

Evidence for substrate effects has been provided in the dependence of unit cell size on alkyl chain length in the series 8CB/10CB/12CB. Close inspection of unit cell size of Fig. 6, a-c, the STM images of the decyl derivative 10CB, reveals a unit cell of 10 molecules — two more than in the case of 8CB. 12CB assumes the 8-molecule unit cell, as with 8CB. This change in unit cell size on minor modification of the molecular length implies that we are dealing with comparable energies for bonding in the substrate and bonding to nearest neighbour molecules. Apparently, the favourable energy of intermolecular interaction is offset by the increasing strain between the substrate and adsorbate every 8 or 10 molecules, depending on the length of the alkyl chains. The difference in adsorption energies between two consecutive members of the series C12-C10-C8-C6 (where the molecular structure of the head group stays fixed and only the length of the alkyl tail changes) can be approximated to be on the order of ~160kJ per unit cell of 8 molecules by applying an approximate value for adsorption energy of ~10kJ per methylene unit.

Among the proposed mechanisms for registration with the substrate are hydrogen atom positioning over graphite rings [4]. Molecular models can be used to illustrate adsorbate registration with the underlying lattice, though one must be wary of carrying bulk

Fig. 6: STM images of 10CB and 12CB on a graphite substrate [4]:

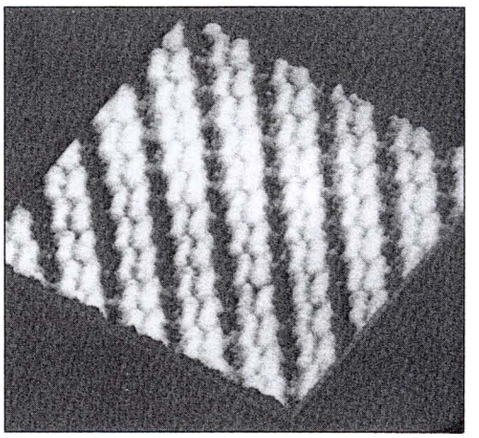

Fig 6a: *(285 x 285Å²) 10 CB, long-range order of smectic planes, side-on.*

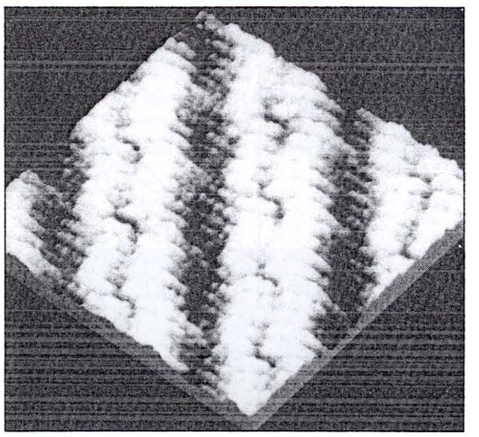

Fig 6b: *(114 x 114Å²) 10 CB, smectic layers resolved as rows of molecules, with 'unit cells' of 10 molecules.*

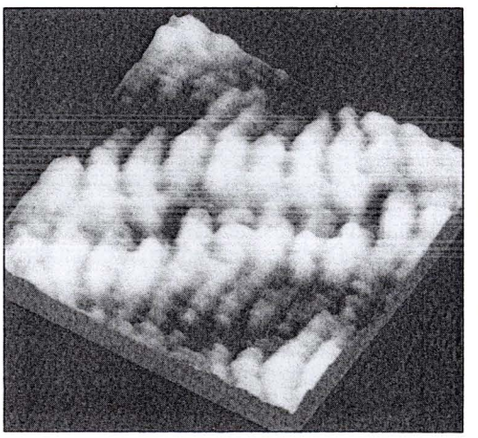

Fig 6c: *(57 x 57Å²) 10 CB, the changing bond angle between tail and head groups is evident on going from the first to the fifth molecule on one side of the unit cell.*

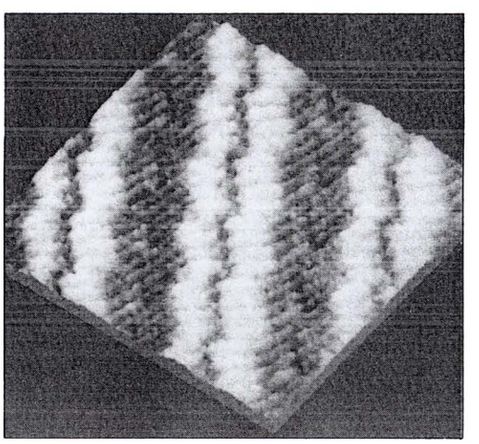

Fig 6d: *(114 x 114Å²) 12 CB, smectic layers resolved as rows of molecules, with 'unit cells' of 8 molecules.*

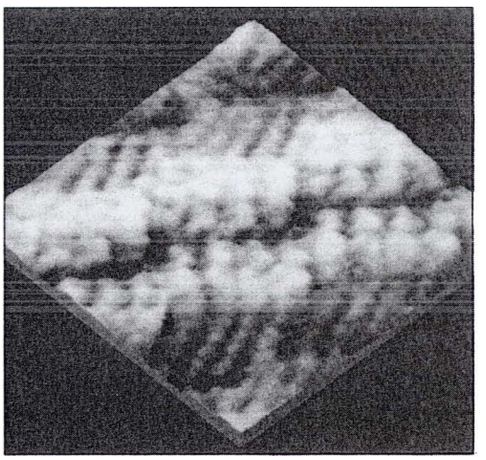

Fig. 6e: (57 x 57Å) 12CB

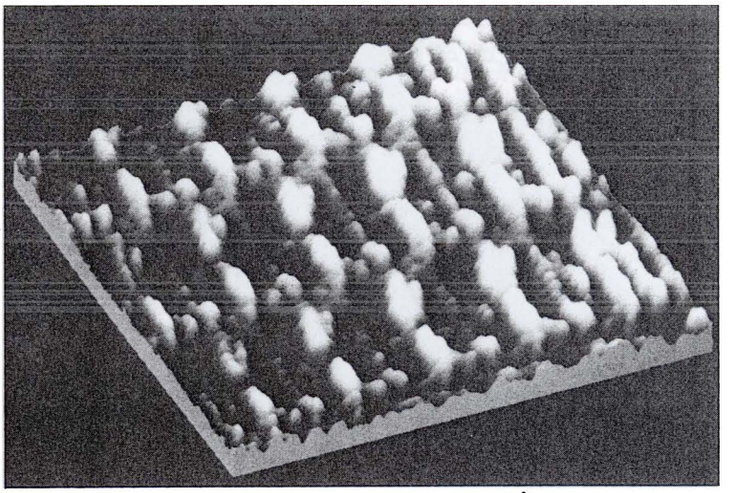

Fig. 9: A rare STM image of 8CB on graphite (105 x 105Å²), with a similar molecular packing pattern observed for 8CB on MoS_2, Fig. 8 [1].

parameters of bond lengths and angles over to the scenario of the interface between the metallic surface and hydrocarbon [1]. Relaxation of these parameters to geometries which are distorted from ground state geometries (as they are known from the bulk or the gas phase) is a factor worth considering, as well as interactions with the image dipole in the underlying substrate.

MoS_2 as a substrate

Dramatic evidence for the influence of the substrate on adsorbate order is provided in the comparison of STM images from two different substrates. The well-studied class of cyanobiphenyl liquid crystals has also been imaged on MoS_2 [7], and the resulting molecular patterns have been compared to those from graphite (Fig. 8). Most striking is the deviation of 8CB's image on MoS_2 from that on graphite. Instead of the long rows of parallel molecules all aligned head-to-head in a row, on MoS_2 a row is made up of a pattern of alternating head-to-head and tail-to-tail parallel dimers. The attractive contacts between rows also come from head-to-head and tail-to-tail interactions. 9CB and 11CB pack similarly on MoS_2 [7]. 10CB and 12CB maintain nearly the same packing pattern on MoS_2 as on graphite. For 10CB, the intermolecular spacing within rows of 10CB molecules is greater on MoS_2 than on graphite: 5.47Å vs. 4.25Å. This is consistent with the larger lattice constant of MoS_2: 3.16Å compared to graphite's 2.46Å.

In many images it appears that adsorbate-substrate interactions dominate intermolecular ones. However, there are a number of counter-examples which don't allow such a clean generalisation. Fig. 9 presents one such exception: 8CB on graphite in a molecular packing pattern more similar to that observed on MoS_2 [1]. 7CB has also been imaged with this molecular packing pattern on graphite [6]. These exceptions imply that this adsorbate system is in a balance between intermolecular and substrate-adsorbate forces, and that a variety of metastable states exist for intermolecular order.

A mixture

In STM images of a binary mixture of 8CB and 12 CB on MoS_2, the two individual components are clearly distinguishable from each other by their different alkyl group lengths (Fig. 10) [8]. The binary mixture takes on the double-row structure observed for 8CB on graphite and for 12CB on graphite and on MoS_2. Close examination of the parallel rows reveals that they are composed of 8CB and 12CB subunits. The ratio of 8CB and 12CB adsorbed on the substrate is different from that in the bulk.

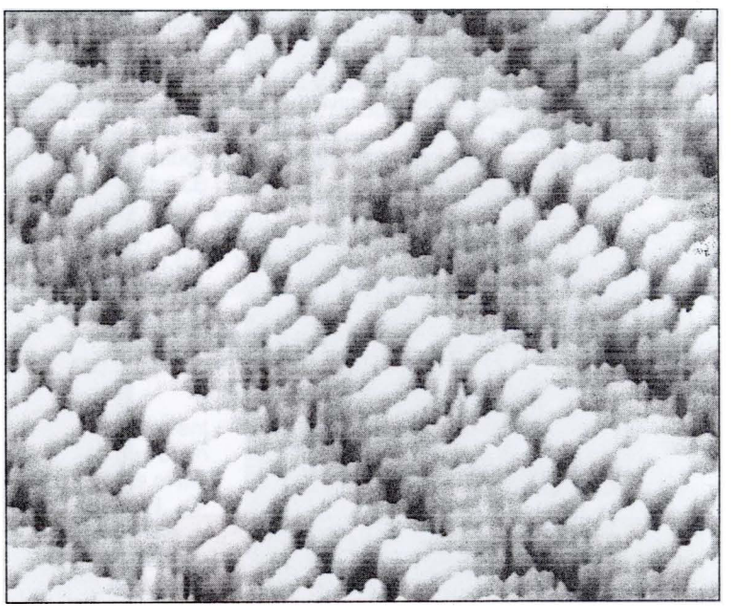

Fig. 10: STM image (100 x 100Å²) (above) and molecular model of a mixture of 8CB and 12CB on a MoS_2 substrate (below) [8].

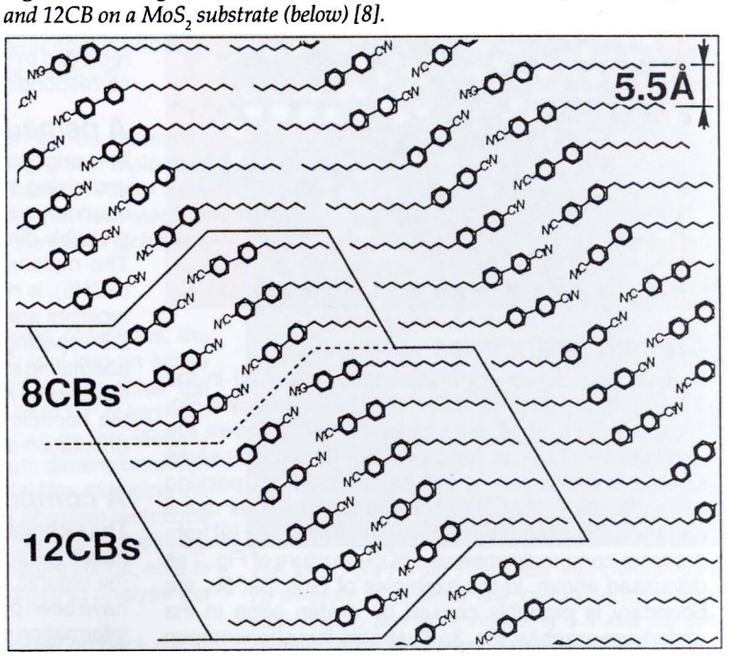

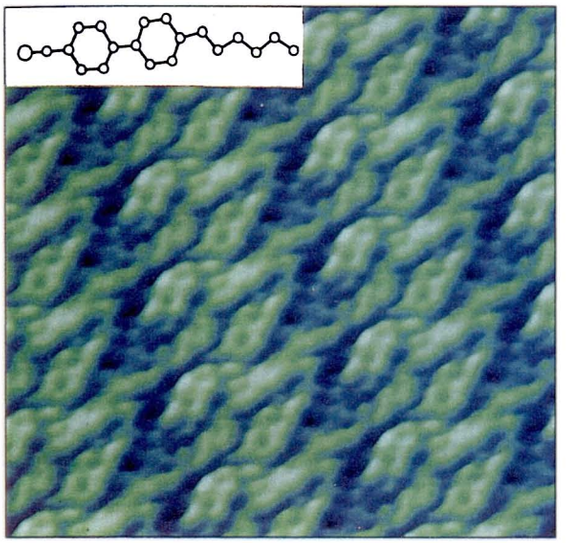

Fig. 7: STM image of 6CB on graphite (70 x70Å²). The ring structure is resolved in every second molecule within a row, interpreted as an alternation between flat-lying and canted biphenyl groups (relative to the flat, underlying graphite substrate).

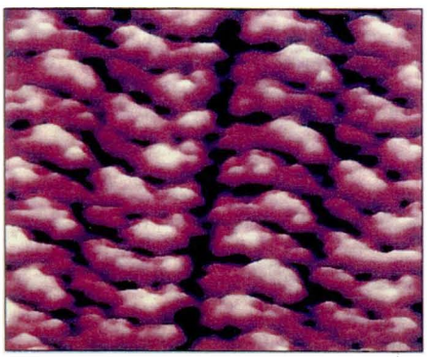

Fig. 8: STM image (80 x80Å²) and molecular model of 8CB on a MoS_2 substrate [7].

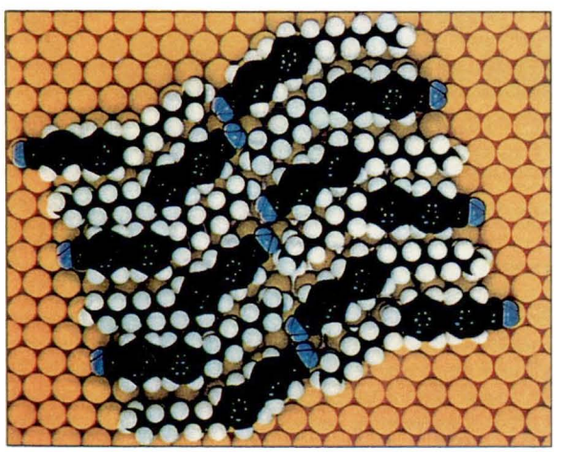

Domain boundaries

Domain boundaries are occasionally observed in the STM images of adsorbates, [1, 9] as seen already in Fig. 3b, an image of 8CB on graphite which shows the termination of smectic rows. Another area on the same sample resolves into a completely different packing pattern for 8CB (Fig. 3c): a moiré pattern. This moiré pattern is one of several examples of deviations [9] from the more commonly observed 8CB structure of Fig. 2 as discussed above. In the examples of Figs. 3a, 3b, the boundary is probably caused by a step edge in the underlying graphite. Fig. 3a illustrates this phenomenon in a particularly good, large-scale image of 10CB

Fig. 12: *AFM images of a 12 bilayer Langmuir Blodgett film of alkoxyphenylester (C_7H_{15}-O-phenyl-phenyl-$COOCH_3$) on hydro-phobised silicon [10].* ***12a:*** *(top) (50 x 50μm²) Overall flat morphology, punctuated regularly with holes that are mostly of one bilayer depth (40Å).* ***Fig. 12b:*** *(bottom) (5 x 5μm²). Smaller scan area of (a).*

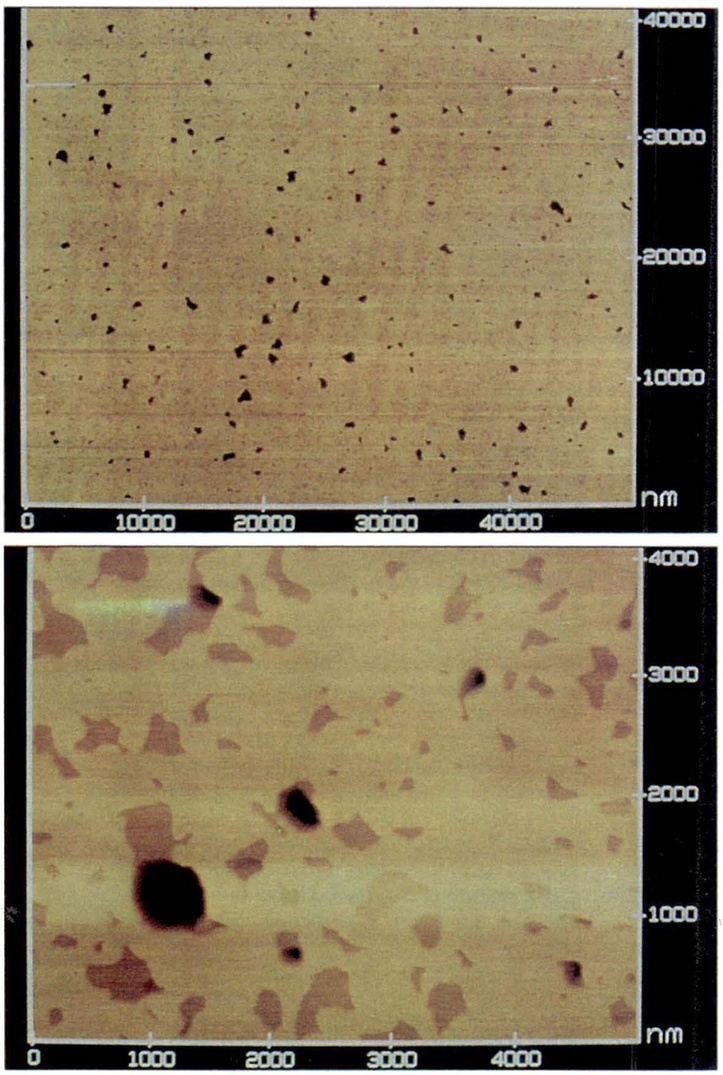

recorded over thousands of angstroms and interrupted by a step of 3.5Å, corresponding to a single layer step of graphite.

A nematic

The origin of the boundary in Fig. 3d is unlikely to be a defect in the underlying substrate, rather an impurity in the overlying adsorbate. The boundary separates the two domains oriented 30° to each other, an angle probably directed by the six-fold symmetry of the underlying graphite. [3] The material in this image, 4-(*trans*-4'*n*-pentylcyclohexyl) benzonitrile (PCH5), is nematic in the bulk at room temperature. Individual molecular moieties are not differentiable in this image, (Fig. 3d) other than a regular 2.5Å spacing between features, a distance typically recorded by STM from alternating methylene groups in alkanes on graphite. The large island-like features have not been identified. An STM image of a continuous plane of the nematic PCH5 is shown in Fig. 11. The common axis of molecular orientation is clearly seen.

A comparative study of film forming techniques

The technique of AFM does not require that the sample be conducting, and hence the surfaces of bulk organics can be studied. Nonetheless, most of the organic materials studied to date by AFM (atomic force microscopy) have been prepared as very thin films. AFM studies have provided thin film information on dimensions not easily accessible, e.g. degrees of coverage as manifested by boundaries, holes and islands, step-heights corresponding

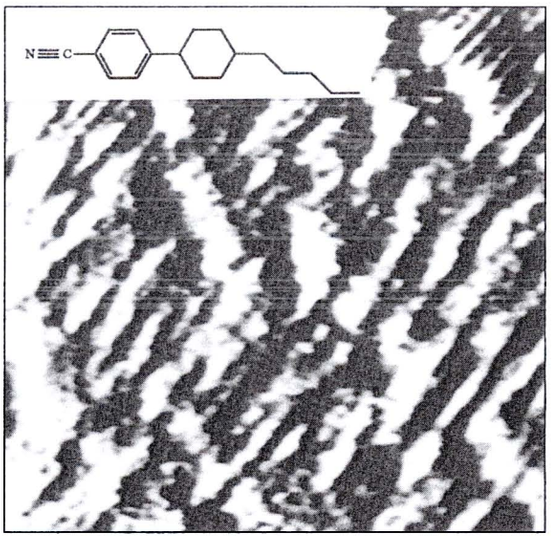

Fig. 11: STM image (160 x 160 Å²) of nematic PCH5 on graphite [3].

to monolayers, bilayers and multilayers, and well-defined interfaces, not only between films and underlying substrates, but also between domains within multicomponent films. [1]

In a study comparing the surface structure of two films from the same class of molecules but prepared by two different techniques, the use of the AFM in tracking qualitative film differences has been demonstrated. The two subjects of this study are Langmuir-Blodgett and freely suspended films. In the first example, the LB technique is used to prepare a 12-bilayer film of liquid crystalline alkoxybiphenylesters [10]. Crystalline films of the heptyl derivative **3**, 4'-n-heptylbiphenyl carboxylic acid methyl ester, [C_7H_{15}-O-phenyl-phenyl-$COOCH_3$] on hydrophobised silicon are analysed. An AFM image (Fig 12) of the surface of the 12-bilayer film shows a continuous flat film interrupted occasionally by holes of a bilayer (40Å) depth: a morphology commonly observed for LB films [1]. A thickness of ~480Å is measured on an edge of the film where both substrate and film are within a single frame.

A very different morphology is observed by AFM for films prepared by a different method: a similar alkoxybiphenylester molecule to that of the LB film has been handled in another manner to produce freely suspended films [10]. Films of the octyl derivative, 4'-*n*-octyloxybiphenyl carboxylic acid ethyl ester, [C_8H_{17}-O-phenyl-phenyl-$COOC_2H_5$], are formed by drawing a thin film of two-dimensional fluid across an aperture at 100°C to create a freely suspended film. The film is then transferred to a hydrophobised substrate, cooled and imaged with the AFM in its crystalline phase. Unlike the previous imaged film, these are hole-free. Large, flat planes, microns in dimension and ~18-22nm (~8 layers) thick are observed, Fig. 13a. These planes are irregularly shaped and overlaid on each other, resembling ice floes. A measured step height of 24Å is consistent with layer spacing from X-ray measurements [10] and corresponds to the length of the molecule.

Molecular resolution

On increasing magnification on one of the broad, flat planes of Fig. 13a, resolution on the scale of individual molecules becomes possible (Fig. 13b). Molecular resolution on one of the flat film planes yields unit cell dimensions of 7.3Å x 5.8Å with an angle of 71° between them. These values differ somewhat from electron diffraction measurements obtained from a film prepared by the same technique from these molecules: 7.8Å x 5.6Å and 90° [10].

Local-scale manipulation

By modifying the cantilever specifications and/or the scanning conditions, the AFM can be transformed from a relatively passive imaging tool into an active modifying tool [1]. When scanning conditions are changed to alter either the applied force or the scan rate (in this specific example, from 10^{-8} to 10^{-7} N and from 0.5μm s^{-1} to 5μm s^{-1}), mono- and multilayer-deep holes can be intentionally introduced into these films. Fig.13c shows areas of 0.5 — 1μm dimension which have been ploughed aside in the top layers of the liquid crystal film, exposing the flat surfaces of underlying layers. Further application of this abrasive technique to lower layers produces multi-tiered holes, until exposing the silicon substrate below. This example illustrates the use of the AFM as a miniature scribe, able to sculpt surfaces on the molecular scale. Studies are in progress to analyse the ability of these micro-sculpted areas to orient adsorbates.

(Concluding remarks and References continued on back page)

Fig. 13: AFM images of freely suspended liquid crystalline film, transferred to a hydrophobised silicon substrate. The molecule, an alkylbiphenylester, is similar to that of the LB film of Fig 12, with minor modification of the substituents (C_8H_{17}-O-phenyl-phenyl-$COOC_2H_5$) [10].

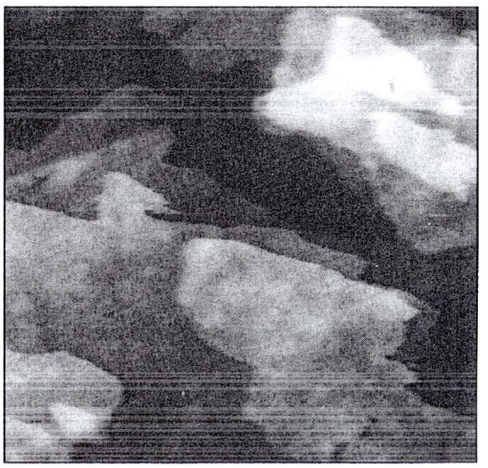

Fig. 13a: (5 x5μm²) Flat, hole-free, irregularly shaped planes of films are imaged. The overall film thickness is ~18-22 nm, corresponding to ~8 layers. Layer steps (24Å) are also measured.

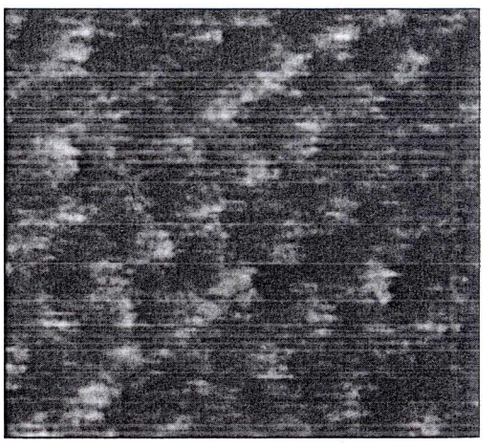

Fig. 13b: (5 x 5 nm²) molecular resolution, from which are measured lattice constants of 7.3Å and 5,8Å with an angle of 71° between them.

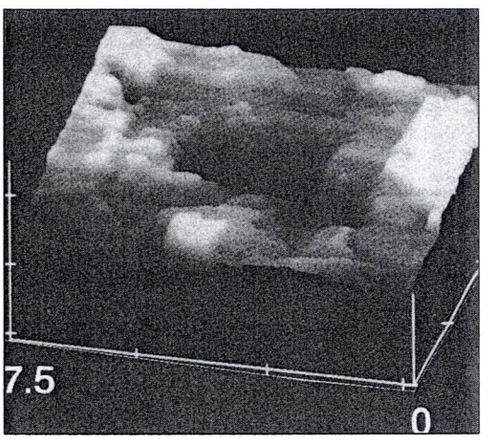

Fig. 13c: (7.5 x 7.5 μm²) 'Sculpted' hole created by the AFM probe. Two-tiered hole created in two stages, sequentially, over scan ranges of 5.0 and 2.5 μm, creating 5 and 14 nm deep holes respectively.

FORTHCOMING MEETINGS

DATE:	CONFERENCE:	VENUE:	CONTACT:
1993			
31 Aug — 3 Sept	Euro Diplay 93 — 13th International Display Research Conference Seminar & Exhibition	Strasbourg, France	*Janine Verdez,* EURODISPLY '93 Secretariat, CNET/LAB/OCM/TEP 22301 LANNION FRANCE FAX: 33-96-05-34-31
18 — 22 Sept	2nd Conference on Liquid Matter	Firenze, Italy	*Dr Marco Zoppi,* Ist. di Elettronica Quantistica, Consiglio Nazionale delle Richerche, Via Pantiatichi, 56/30 1-50127 FIRENZE, ITALY Fax: 39-55-414612
27 Sept — 1 Oct	Europhysics Conference on Macromolecular Physics 1993: Transitions in Oligomer & Polymer Systems	Ulm, Germany	*Prof Dr H G Kilian,* Universität Ulm, Experimentelle Physik, Albert-Einstein Allee 11, D-7900 ULM, GERMANY FAX: 49-731-502-3036
28 Sept — 1 Oct	FLC '93, Tokyo: Fourth International Conference on Ferroelectric Liquid Crystals	Tokyo, Japan	*Prof Atsuo Fukuda,* Tokyo Inst. of Tech., Faculty of Engineering, Dept of Org. & Polymeric Materials, O-okayama, Meguro-ku, Tokyo 152, JAPAN Fax: 81-3-3748-5369
4 — 8 October	V International Meeting on Optics of Liquid Crystals	Lake Balaton, Hungary	*Dr I Janossy,* Central Research Inst. for Physics, H-1525 BUDAPEST 114, PO Box 49, HUNGARY Fax: 36-1-169-5380
1994			
3 — 8 July	15th ILCC: 15th International Liquid Crystal Conference	Budapest, Hungary	*Dr Agnes Buka,* Research Institute for Solid State Physics, Hungarian Academy of Sciences, H-1525 BUDAPEST, PO Box 49, HUNGARY Fax: 36-1-169-5380
6 — 9 September	International conference on Liquid Crystal Polymers	Beijing, P R China	*Dr X J Wang,* Beijing ERC of LC Technology & Dept of Chemistry, Tsinghua University BEIJING 100084, P R CHINA FAX: 86-1-2564372

Concluding remarks on the impact of STM and AFM on our knowledge of liquid crystals

The STM and AFM are able to provide information about molecular environments not directly observed before, on both the intermolecular and intramolecular scales. From the STM one obtains atomic topography when electronic structure coincides with atomic structure. From the AFM one obtains maps of molecular topography when local material properties, such as elasticity, coincide with molecular structure.

Both the STM and AFM are still in a stage of continuous development and change, However future developments will rely in large part on the input from other scientific disciplines, such as catalysis, optics, tribology and surface science. Significant advances will be made when scientists from outside the field of STM and AFM pose their own scientific challenges to operators of these instruments, within collaborative studies, to arrive at a common goal of understanding molecular behaviour.

Acknowledgements

Images, data and collegial interactions were gracefully provided for this article by John Foster, Doug Smith, Wolfgang Heckl, Masahiko Hara, Dario Anselmetti, René Overney, and Gero Decher.

References

[1] A review of STM and AFM to organic materials that includes background information, extensive references, and broad coverage of liquid crystals: J Frommer, *Angewandte Chemie*, International Edition, English, **Vol 31**, pp 1298-1328 (1992).

[2] J Spong, L LaComb, M Dovek, J Frommer, *J. de Phys.*, **50** (1989), 2139.

[3] J Foster, J Frommer, *Nature*, **333**, (1988), 542.

[4] D Smith, H Hörber, C Gerber, G Binnig, *Science*, **245** (1989), 43; D Smith, J Hörber, G Binnig, H Nejoh, *Nature*, **344** (1990), 641.

[5] G Brownsey, A Leadbetter, *Phys. Rev. Lett.*, **44**, (1980) 1608; A Leadbetter, J Frost, J Gaughan, G Gray, A Mosley, *J. de Phys. France*, **40**, (1979) 375.

[6] W Mizutani, M Shigeno, Y Sakakibara, K Kajimura, M Ono, S Tanishima, K Ohno, N Toshima, *J. Vac. Sci. Technol. A*, **8**, (1990), 675.

[7] Y Iwakabe, M Hara, K Kondo, K Tochigi, A Mukoh, A Yamada, A Garito, H Sasabe, *Jpn. J. Appl. Phys.*, **30**, (1991), 2542; *ibid*, **29** (1990), L2243; M Hara, Y Iwakabe, K Tochigi, H Sasabe, A Garito, A Yamada, *Nature*, **344**, (1990), 228.

[8] Y Iwakabe, M Hara, K Kondo, S Oh-hara, A Mukoh, H Sasabe, *Jpn. J. Appl. Phys.*, **31**, (1992), L1771.

[9] J Foster, J Frommer, J Spong, *Proc. SPIE*, **1080**, (1989), 200; D Smith, *J. Vac. Sci. Technol. B*, **9**, (1991), 1119.

[10] R Overney, E Meyer, J Frommer, H Güntherodt, G Decher, J Reibel, U Sohling, *Langmuir*, **9**, (1993), 341. ❑

Published by the International Liquid Crystal Society *Typeset and designed by Freelance Media Services*
Printed by Eastwood Press Ltd, Midland Road, Rotherham, S61 1SZ, UK